

# An Experimental and Analytical Study on the Seismic Performance of Piers with Different Foundation Bottom Widths

Takashi Nagao

Research Center for Urban Safety and Security  
Kobe University  
Kobe City, Japan  
nagao@people.kobe-u.ac.jp

Yoshinao Kurachi

Technical Division  
Oriental Shiraishi Corporation  
Tokyo, Japan  
yoshinao.kurachi@orsc.co.jp

Received: 17 May 2022 | Revised: 19 July 2022 | Accepted: 21 July 2022

**Abstract**-Piers can be severely damaged by earthquakes. When an action of a massive earthquake is assumed, the seismic performance of the pier can be improved by widening the foundation width. A previous horizontal loading study indicated that extending only the Foundation Bottom (FB) width, rather than the complete foundation, can boost seismic resilience while suppressing the increase in building cost. However, the research dealt with only two types of FB width, i.e. normal and widened, and the data for sufficiently assessing the inclination angle of the pier with loading were not obtained. In this study, to evaluate the seismic performance of piers with different FB widths in more detail, horizontal loading tests on piers with ordinary columnar foundations and two types of piers with widened FB were conducted, and the seismic resistance of the three pier types were compared. It was shown that horizontal displacement and inclination angle of the pier can be reduced by widening the FB. Furthermore, finite element analysis was carried out to reproduce the experimental results. The analysis results showed good agreement with the experimental results in terms of pier horizontal displacement and inclination angle.

**Keywords**-pier; foundation; seismic performance; finite element analysis

## I. INTRODUCTION

The pier is a major port structure that facilitates cargo shipping. Since the pier is generally constructed on the soft ground in the coastal area, it can be damaged by earthquakes [1, 2]. Due to the enlargement of ships, the pier is required to be deeper in water depth, which brings about an increase in seismic load. In addition, a considerable lateral spreading pressure may act during a massive earthquake, which seismic design codes [3, 4] do not adequately account for [5]. Furthermore, the pier is strongly influenced by the ground deformation during earthquakes and undergoes residual displacement [6, 7], even when the structural member is not injured [8]. As a result, from the viewpoint of evaluating the serviceability of the pier, residual displacement needs to be assessed with high accuracy along with structural member safety. When the seismic resistance of the pier is insufficient against the reference earthquake, the cross-sectional width of

the foundation is increased to improve the seismic resistance in design practice, but the increase of the foundation width leads to a drastic increase in the construction cost. When a broad foundation is employed, the vertical subgrade reaction operating at the Foundation Bottom (FB) generates rotational resistance moment opposing the inclination of the pier. However, it should be noted that the subgrade reaction modulus decreases with increasing foundation width [9, 10]. As a way to increase the seismic resistance of the pier while keeping the rise of the construction cost mild, a method of widening only the FB was suggested in a previous study [11], and the horizontal loading test showed that the seismic performance is improved by widening the FB. However, in the previous study, only two varieties of FB width were handled, namely normal and widened, and data for adequately measuring the inclination angle of the pier with loads were not collected. In addition, there is no seismic design method that evaluates the seismic performance of a FB widened pier at the moment. In the current research, in order to assess the seismic performance of piers with different FB widths in more detail, new horizontal loading tests on piers with ordinary columnar foundations and two types of pier with widened FB were performed and the seismic resistance of the models was studied. Furthermore, for the development of the seismic design method of the FB widened pier, the findings of the experimental results were reproduced with two-dimensional Finite Element Analysis (FEA) and the reproducibility of the experimental results was demonstrated.

## II. METHOD

Horizontal loading experiments of the pier using a mega torque motor were performed. Steel rigid frame models imitating piers with 150mm depth were put in the ground in a soil tank 900mm wide and 500mm deep (Figure 1). These dimensions were set considering the ease of performing the experiment and to prevent the bottom slab of the soil tank from suppressing the settlement of the pier foundation with loading. The pier model was installed in the central part of the soil tank in the depth direction to avoid the effect of ground confinement by the side wall of the soil tank. A steady brace was fitted to

Corresponding author: Takashi Nagao

prevent the pier model from tilting in the soil tank depth direction with loading. Figure 2 demonstrates the specifications of the model. A circular cross-section of 120mm in diameter was employed as the normal type, and pier models with the same shape of the column, FBs of 180mm in width and 120mm in depth were used as the widened 1 type, and FBs of 240mm in width and 120mm in depth were used as the widened 2 type. In the previous study [11], the scaling factor (prototype/model) was 100, whereas in this study, a reduced scaling factor of 50 was attained. The normal model weighs 20.145kg, the widened 1 model weighs 25.145kg, and the widened 2 model weighs 28.635kg.

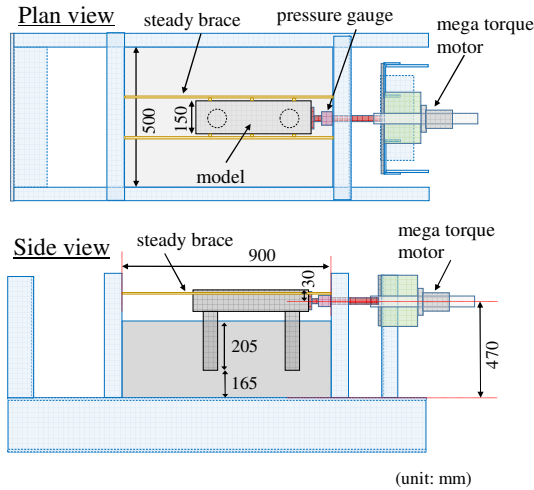


Fig. 1. Soil tank.

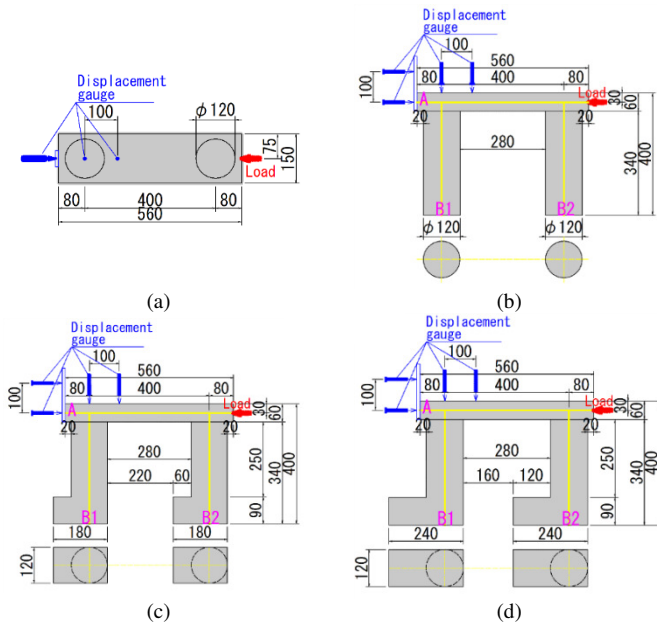


Fig. 2. Model specifications (unit: mm): (a) plan view, (b) side view: normal, (c) side view: widened 1, and (d) side view: widened 2.

The ground was prepared by air pluviation. Tohoku Silica Sand No. 6 in dry state was used. The target relative density of the ground was 77% which corresponds to the dense ground

condition. The foundation of the true pier is embedded into the bedrock to support the structure's weight. To simulate this situation, loading tests and shake table tests have often been performed in which the FB was fixed to the soil tank [12-16]. However, in such cases, the constraint of the FB due to the bedrock is excessively expressed, leading to no settlement or inclination of the foundation due to loading. The bedrock is a very rigid ground, but it slightly deforms when a load is applied from the FB, therefore, the pier is inclined during an earthquake. In this experiment, the FB of the pier model was not fastened to the soil tank but was put at a height of 165mm from the bottom end of the soil tank. The ground's thickness was 370mm. The loading was applied at a constant displacement speed of 1.3mm/s and the greatest displacement was 20mm, which is equivalent to 7m on a real scale by similitude [17] based on the scaling factor. The horizontal and vertical displacements of the pier and horizontal load were captured with a data logger. Displacement gauges were attached to the model superstructure to measure horizontal and vertical displacements. In [11], horizontal and vertical displacements were evaluated by one displacement gauge respectively. As a result, the displacement and inclination angle of the pier could not be accurately measured. In this research, horizontal and vertical displacements were evaluated by two displacement gauges. Noise in the observed data was eliminated similarly to [11] by executing fast Fourier transform and inverse fast Fourier transform after multiplying with a low-pass filter at 1Hz.

III. EXPERIMENTAL RESULTS

The time history of the loading of each case is depicted in Figure 3. In about 10 seconds after loading, the value of load decreased in each case. Because the loading was done at a constant displacement speed, the pier's displacement is progressing with decreasing load after roughly 10 seconds. This is because the main displacement mode of the pier changed from the inclination at the early stage of loading to the sliding in the latter half of loading.

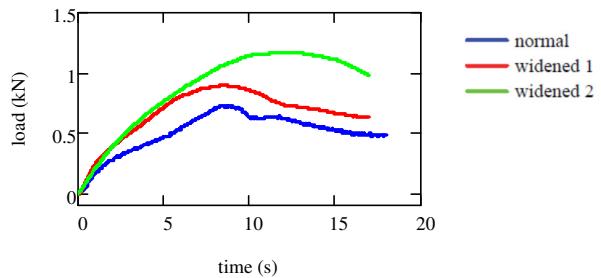


Fig. 3. Time history of load.

As previously stated, this test does not fix the FB of the pier to the soil tank, therefore, sliding happens in the pier. Since the FB of the actual pier is embedded into the bedrock, tilting of the pier occurs when lateral load is applied, but not sliding. Following that, we will focus on the results of the first half of loading. Based on the data of the four displacement gauges, the horizontal displacement at point A of the superstructure and

point B1 of the FB illustrated in Figure 2, and the inclination angle of the pier were determined (Figure 4). The tendency differs between the normal and widened types in the early stages of loading, although there is no significant variation in displacements between the two widened types. For the same load, the horizontal displacements at the FB (point B1) are almost the same, while the horizontal displacement of the superstructure (point A) is significant in the normal type and modest in the widened types. For this reason, the inclination angle of the normal type is larger than that of the widened types.

Figure 5 illustrates the piers' displacements when the load was 0.69kN, which was the maximum load observed for the normal type. Here, the displacements are magnified by a factor of 10. Both the horizontal displacement and inclination are large in the order of normal, widened 1, and widened 2 types. The horizontal displacements are 8.54, 4.84, and 4.28mm respectively and the inclination angles are 0.017, 0.008, and 0.006rad respectively. In the previous study [11], the widened type showed approximately 1/3 times the horizontal displacement compared with the normal type. In this study, the widened types have 1/2–1/3 times the horizontal displacements and 1/2 times the inclination angles compared with the normal type.

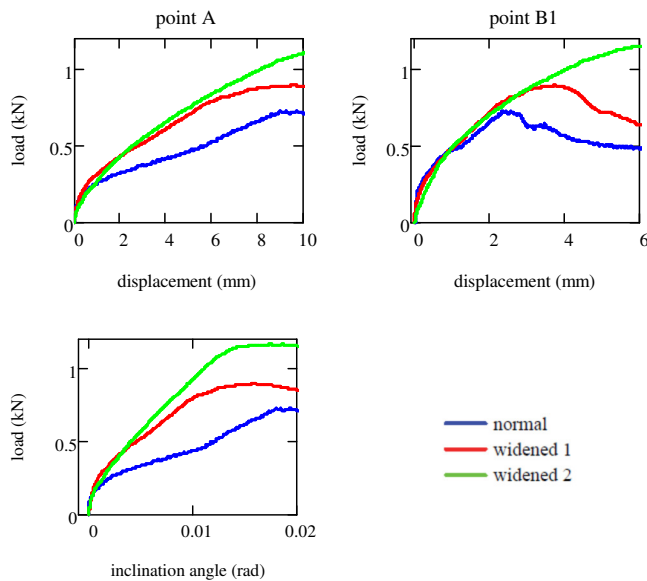


Fig. 4. Horizontal displacement and inclination angle.

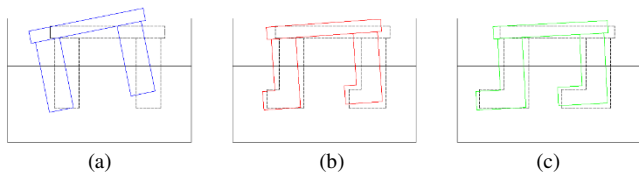


Fig. 5. Displacement of piers: (a) normal, (b) widened 1, (c) widened 2.

As was discussed in [10], when the FB is widened, the Rotational Resistance Moment (RRM) caused by the subgrade reaction acting at the FB surface increases and the shear

deformation at the soil under the FB decreases. In addition, as was discussed in [11], in the widened type, the rotational center is closer to the center of the superstructure when compared with the normal type, therefore, RRM arm length is larger than in the normal type. Those are the major reasons of the high seismic resistance of the FB widened pier when compared with the normal type. The variation in the seismic resistance of the two widened types is remarkable in the range where the horizontal displacement of the superstructure (point A) exceeds 6mm, which is equivalent to 2.1m on the real scale by the similitude [17]. The allowable displacement for quay wall during an earthquake is 1m or less in the seismic design code [6], therefore, this amount of displacement is greater than what is permitted in seismic design. As a result, widening the FB to 1.5 times the width of the foundation column would be sufficient to improve the seismic resilience of the pier.

#### IV. FINITE ELEMENT ANALYSIS

##### A. Analytical Method

Two-dimensional FEA was performed to reproduce the experimental results. The analysis code employed is FLIP [18], by which the seismic responses of port structures such as piers have been evaluated [8, 19]. The code employs a multi-spring model [20] to express the ground response under principal stress axes rotation. The nonlinearity of the ground is expressed as (1) using a hyperbolic model [21].

$$\frac{G}{G_0} = \frac{1}{1 + G_0 \gamma / \tau_m} \quad (1)$$

where  $G$  is the shear rigidity,  $G_0$  is the initial shear rigidity,  $\gamma$  is the shear strain, and  $\tau_m$  is the shear strength, which is calculated by [22]:

$$\tau_m = \sigma_m' \sin \phi \quad (2)$$

where  $\sigma_m'$  is the effective confining pressure and  $\phi$  is the shear resistance angle.

The shear resistance angle of the ground is calculated using the relative density by referring to [22]. The ground shear rigidity  $G_m$  at each depth is calculated by [23]:

$$G_m = G_{ma} \left( \frac{\sigma_m'}{\sigma_{ma}'} \right)^{0.5} \quad (3)$$

where  $G_m$  is the shear rigidity,  $G_{ma}$  is the reference shear rigidity,  $\sigma_m'$  is the effective confining pressure, and  $\sigma_{ma}'$  is the reference effective confining pressure corresponding to the reference shear rigidity.

The shear rigidity of the ground is calculated by (4) using Young's modulus. Based on the results of a separate compression experiment, the Young's modulus was determined to be 2437kPa at the center depth of the ground.

$$G_m = \frac{E_m}{2(1+\nu)} \quad (4)$$

where  $E_m$  is the Young's modulus,  $G_m$  is the shear rigidity, and  $\nu$  is the Poisson's ratio.

The superstructure and foundations of the pier are modeled by linear beam elements, and the variation in weights of each pier is expressed by changing the density of the foundation elements. Because the ground above the FB is assumed to act integrally with the pier in the widened types, the influence is accounted for in the foundation element densities. Tables I and II indicate the parameters of the ground and pier, respectively.

TABLE I. GROUND PARAMETERS

$\sigma_{ma}$ (kPa)	2.06
$G_{ma}$ (kPa)	916.2
$\rho$ (t/m <sup>3</sup> )	1.483
$\phi$ (°)	41.2
$\nu$	0.33

$\rho$ : density

TABLE II. PIER PARAMETERS

	Superstructure	Foundation		
		Normal	Widened 1	Widened 2
$G$ (kPa)		7.69×10 <sup>7</sup>		
$\nu$		0.33		
$\rho$ (t/m <sup>3</sup> )	2.624	0.827	2.172	3.112
$A$ (m <sup>2</sup> )	0.0090	0.0113		
$I$ (m <sup>4</sup> )	2.70×10 <sup>-6</sup>	1.02×10 <sup>-5</sup>		

$\rho$ : density,  $A$ : area,  $I$ : moment of inertia

Soil-spring elements were arranged at the boundary between the foundation and the ground except for the FB. In two-dimensional analysis, this element reproduces the effect of the soil slipping through the columnar foundations with loading, and the soil-spring force estimated using (5) is proportional to the ratio of the soil's shear stress increment to shear strain increment ( $d\tau/d\gamma$ ).

$$k_h = \alpha d\tau / \beta d\gamma \quad (5)$$

where  $k_h$  is the soil-spring modulus and  $\alpha$  and  $\beta$  are the coefficients decided following the diameter and spacing of the foundation.

Since the soil elements exhibit nonlinear characteristics, the spring force reflects the effect of the decrease in the soil rigidity with loading. A frictional resistance force equivalent to the initial shear rigidity of the ground acts in the axial direction of the foundation until the shear stress reaches shear strength. At the FB, nonlinear spring elements with rigidity in three directions, i.e. axial spring, perpendicular to axial spring (shear spring), and rotational spring, are arranged. The axial spring's characteristic is defined as the relationship between the axial spring force and displacement difference. When the node of the FB is placed below the node of the ground element in contact with the FB, the displacement difference is described as negative. The subsidence of the FB is always accompanied by the same amount of subsidence of the ground due to loading; therefore, the displacement difference is not negatively generated. As a result, it was set to form a very large axial spring force when the displacement difference is in the negative range. In contrast, a positive displacement difference

corresponds to the circumstance in which the FB on the loading side floats up while the pier is inclined. Because there is no tensile force acting between the FB and the ground at that moment, the axial spring force is adjusted to practically zero when the displacement difference is positive. The shear spring expresses the sliding of the pier. First, maximum static friction force was assessed by assuming the friction coefficient between pier FB and the ground to be 0.5. The shear spring stiffness was set to be: (1) as much as the shear rigidity of the ground when the shear force was less than 0.5 times the maximum static friction force, (2) half of the shear rigidity of the ground when the shear force was 0.5–1.0 times the maximum static friction force, and (3) 5% of the shear rigidity of the ground when the shear force was more than the maximum static friction force. The rotational spring is bilinear, and the parameters were chosen to create the RRM in accordance with the FB width, as described in [10]. Figure 6 depicts the nonlinear spring elements' properties.

Figure 7 shows the FE mesh around the pier model. The soil mesh measures 15mm in height and 50mm in width. To account for the difference in ground rigidities in the vertical direction, the ground was divided into two elements: the top layer colored orange and the lower layer colored green, although the same parameters were applied to both soil elements. The side and bottom surface boundary conditions were designed to be fixed boundaries.

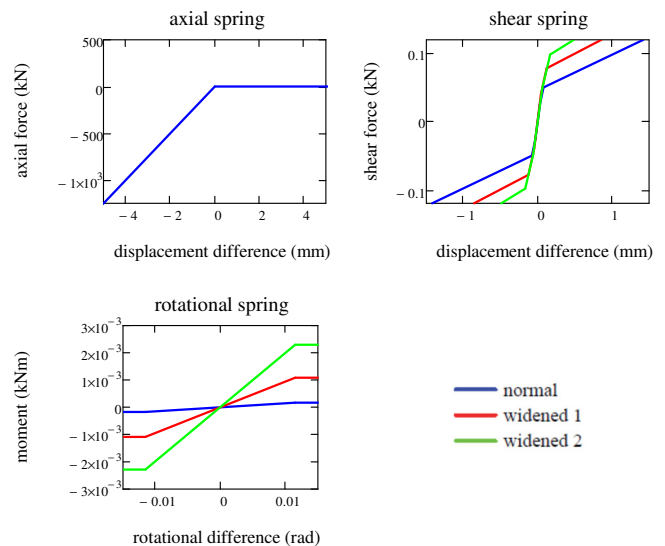


Fig. 6. Characteristics of nonlinear springs.

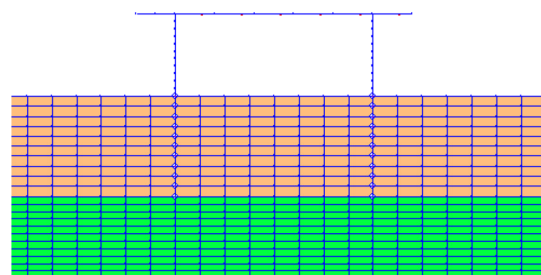


Fig. 7. FE mesh.

B. Analysis Results

Figure 8 compares the analysis results with the experimental results on the horizontal displacement of the superstructure (point A), vertical displacements of the FB (points B1 and B2), and inclination angle for the normal type. When settlement occurs, the vertical displacement is defined as negative. Early in the loading stage, the analytical findings of points A, B1, B2, and inclination angle showed fairly high agreement with the experimental data. However, they tended to be somewhat underestimated. In the latter half of the loading, the analysis results of the displacement and the inclination angle increased rapidly, and the deviation from the experimental results is large, because loading increased the shear stress of the soil element in contact with the FB, and the shear strain rose suddenly in the later part of loading due to the impact of the ground's nonlinear properties. Figure 9 depicts the time histories of vertical strain and shear strain of the soil element in contact with the FB (point B1). The normal strain grows steadily over time, but shear strain increases drastically when displacement and inclination in Figure 7 increase rapidly.

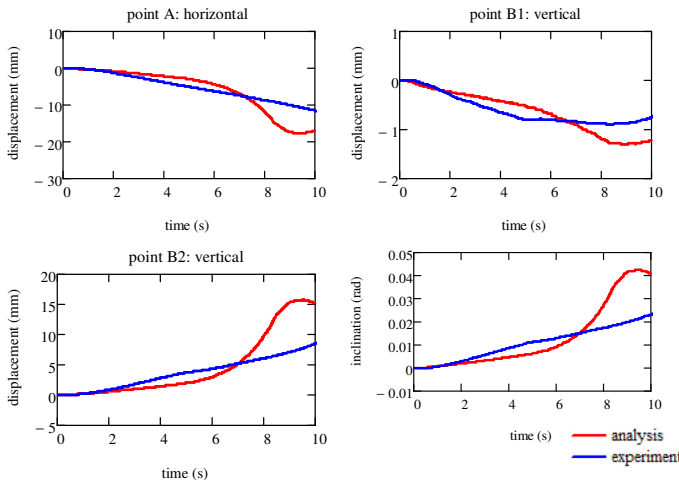


Fig. 8. Analysis results (normal type).

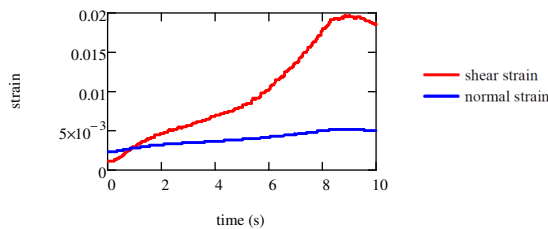


Fig. 9. Ground strain.

C. Discussion

The cause of the mismatch between the analysis and the experimental results in the latter half of loading is discussed in this section. In this analysis, the foundation is treated as a beam element with no breadth, such that the pier load operates as a concentrated load on the ground element in contact with the FB. As a result, the shear stress in the soil element tends to be overestimated. Because the FB has a width, a distributed load is

given to the ground, making the effect of ground nonlinearity unlikely to be realized. To enhance the reproducibility of the experimental results, this paper changes to an elastic element in which nonlinearity does not occur on the soil element below the FB. Figure 10 depicts the analysis findings. The FB subsidence understates the experimental results slightly since soil materials at the foundation's bottom edge do not exhibit nonlinear behavior, but reproducibility is greatly improved for horizontal displacement, vertical displacement, and pier inclination angle.

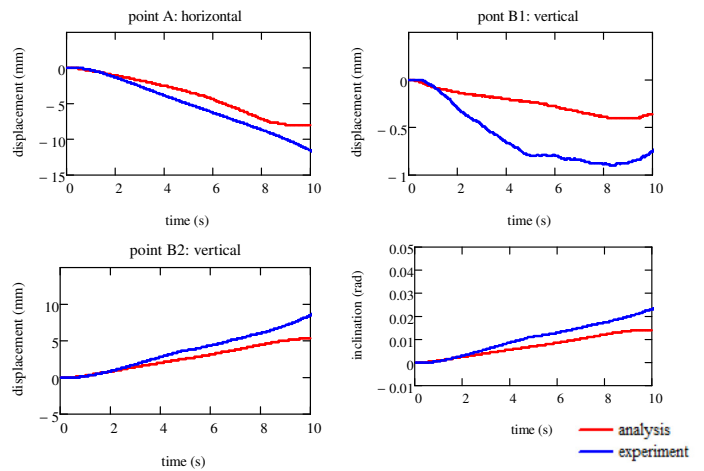


Fig. 10. Analysis results (normal type)/

Figures 11 and 12 demonstrate the analysis results of widened 1 and widened 2 types respectively using the soil element below the FB as an elastic element. Because the FB is wider in the widened types, it floats with loading at point B1, but this phenomenon cannot be recreated in the analysis because the foundation is modeled by beam elements. However, the floating of point B2 at the FB on the loading side is well reproduced, and the inclination of the superstructure (point A) is also very well reproduced. As a result of referring to the modeling in this study, it can be determined that accurate analysis can be carried out for the seismic response of the pier whose foundation is embedded into stiff ground.

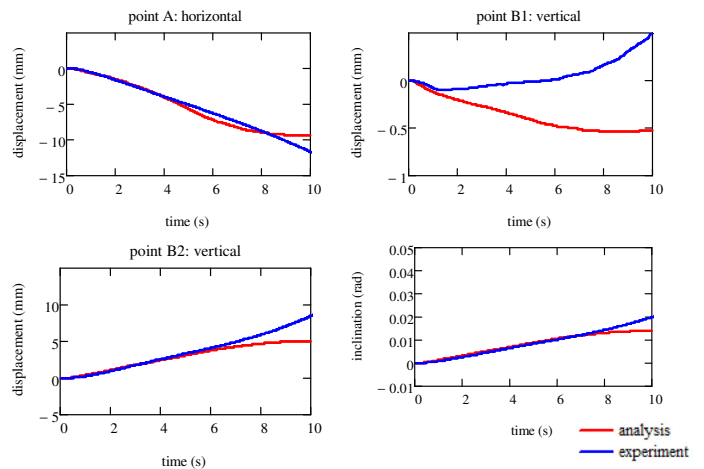


Fig. 11. Analysis results (widened 1 type).

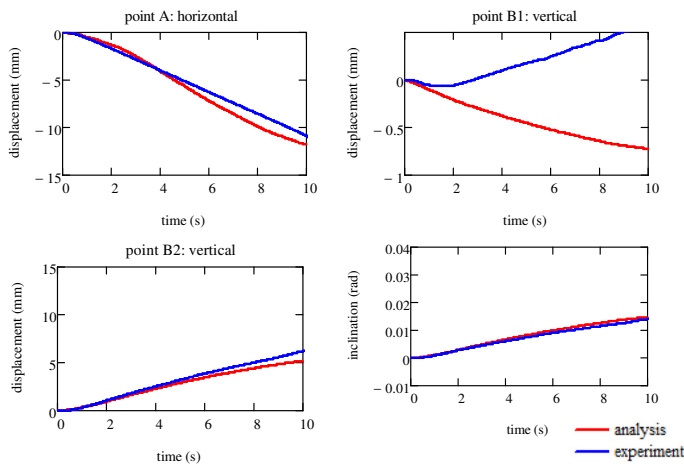


Fig. 12. Analysis results (widened 2 type).

## V. CONCLUSION

In this study, in order to evaluate the seismic performance of piers with different FB widths in more detail, horizontal loading experiments for the pier with an ordinary columnar foundation and two types of the pier with widened FB were performed, and the seismic resistance difference of the three pier types was compared from the viewpoint of horizontal displacement and inclination angle. Two-dimensional FEA was used to replicate the experimental results, and the reproducibility of the experimental results was studied. The main conclusions obtained by this study are:

- Regarding the seismic performance of three pier types in which the FB width differs, there are large variations in the seismic performance between the normal type and the widened FB types, and displacement and inclination of the pier can be reduced by widening the FB. Because there is no significant difference in seismic performance between the two widened types within the range of displacement allowed in seismic design, it is recommended that the FB width should be about 1.5 times the foundation width of the columnar part to improve seismic performance while keeping the increase in construction cost to a minimum.
- The two-dimensional FEA modeling of the ground and pier enables us to evaluate accurately the response of the pier during horizontal loading. To avoid overestimating the shear strain produced in the ground at the FB when modeling the foundation with beam elements, the ground below the FB should be modeled as an elastic body, whereas nonlinearity should be considered for the ground above it. A suitable parameter setting approach for the spring element to be deployed at the soil-foundation boundary was presented. These findings pave the way for a rational seismic design method of the pier with widened FB.

## ACKNOWLEDGMENTS

The authors are grateful to Yohei Ninomiya and Ryota Tsubata for their help in carrying out the experiments.

## REFERENCES

- [1] S. Werner, N. McCullough, W. Bruin, A. Augustine, G. Rix, B. Crowder, and J. Tomblin, "Seismic Performance of Port de Port-Au-Prince during the Haiti Earthquake and Post-Earthquake Restoration of Cargo Throughput", *Earthquake Spectra*, Vol. 27, No. S1, pp. 387–410, Oct. 2011, <https://doi.org/10.1193/1.3638716>.
- [2] T. Sugano, A. Nozu, E. Kohama, K. Shimosako, and Y. Kikuchi, "Damage to coastal structures", *Soils and Foundations*, Vol. 54, No.4, pp. 883–901, Aug. 2014, <https://doi.org/10.1016/j.sandf.2014.06.018>.
- [3] *Seismic Design of Piers and Wharves, ASCE/COPRI 61-14*, American Society of Civil Engineers, 2014.
- [4] *Technical standards and commentaries for port and harbour facilities in Japan*, Ports and Harbours Bureau, Ministry of Land, Infrastructure, Transport and Tourism, National Institute for Land and Infrastructure Management, Port and Airport Research Institute, The Overseas Coastal Area Development Institute of Japan, 2009.
- [5] T. Nagao and D. Shibata, "Experimental Study of the Lateral Spreading Pressure Acting on a Pile Foundation During Earthquakes", *Engineering, Technology & Applied Science Research* Vol. 9, No. 6, pp. 5021-5028, Dec. 2019, <https://doi.org/10.48084/etasr.3217>.
- [6] J. W. Yun and J. T. Han, "Dynamic behavior of pile-supported wharves by slope failure during earthquake via centrifuge tests", *International Journal of Geo-Engineering*, vol. 12, Nov. 2021, Art. no. 33, <https://doi.org/10.1186/s40703-021-00161-4>.
- [7] L. Su, J. Lu, A. Elgamal, and A. K. Arulmoli, "Seismic performance of a pile-supported wharf: Three-dimensional finite element simulation", *Soil Dynamics and Earthquake Engineering*, Vol. 95, pp. 167-179, Apr. 2017, <https://doi.org/10.1016/j.soildyn.2017.01.009>.
- [8] T. Nagao and P. Lu, "A simplified reliability estimation method for pile-supported wharf on the residual displacement by earthquake", *Soil Dynamics and Earthquake Engineering*, vol. 129, Feb. 2020, Art. no. 105904, <https://doi.org/10.1016/j.soildyn.2019.105904>.
- [9] T. Nagao, "Effect of Foundation Width on Subgrade Reaction Modulus", *Engineering, Technology & Applied Science Research* Vol. 10, No. 5, pp. 6253-6258, Oct. 2020, <https://doi.org/10.48084/etasr.3668>.
- [10] T. Nagao and R. Tsubata, "Evaluation Methods of Vertical Subgrade Reaction Modulus and Rotational Resistance Moment for Seismic Design of Embedded Foundations", *Engineering, Technology & Applied Science Research* Vol. 11, No. 4, pp. 7386-7392, Aug. 2021, <https://doi.org/10.48084/etasr.4269>.
- [11] T. Nagao, "An Experimental Study on the Way Bottom Widening of Pier Foundations Affects Seismic Resistance", *Engineering, Technology & Applied Science Research* Vol. 10, No. 3, pp. 5713-5718, Jun. 2020, <https://doi.org/10.48084/etasr.3590>.
- [12] J. A. Knappett and S. P. G. Madabhushi, "Influence of axial load on lateral pile response in liquefiable soils, Part I: Physical modelling", *Geotechnique*, Vol. 59, No. 7, pp. 571-581, Sep. 2009, <https://doi.org/10.1680/geot.8.009.3749>.
- [13] D. Lombardi and S. Bhattacharya, "Evaluation of seismic performance of pile-supported models in liquefiable soils", *Earthquake Engineering & Structural Dynamics*, vol. 45, pp. 1019–1038, Feb. 2016, <https://doi.org/10.1002/eqe.2716>.
- [14] L. Su, L. Tang, X. Ling, C. Liu, and X. Zhang, "Pile response to liquefaction-induced lateral spreading: a shake-table investigation", *Soil Dynamics and Earthquake Engineering*, Vol. 82, pp. 196-204, Mar. 2016, <https://doi.org/10.1016/j.soildyn.2015.12.013>.
- [15] G. Li and R. Motamed, "Finite element modeling of soil-pile response subjected to liquefaction-induced lateral spreading in a large-scale shake table experiment", *Soil Dynamics and Earthquake Engineering*, vol. 92, pp. 573-584, Jan. 2017, <https://doi.org/10.1016/j.soildyn.2016.11.001>.
- [16] J. W. Yun and J. T. Han, "Dynamic behavior of pile-supported wharves by slope failure during earthquake via centrifuge tests", *International Journal of Geo-Engineering*, vol. 12, no. 33, Nov. 2021, <https://doi.org/10.1186/s40703-021-00161-4>.
- [17] S. Iai, "Similitude for Shaking Table Tests on Soil-Structure-Fluid Model in 1g Gravitational Field," *Soils and Foundations*, vol. 29, no. 1, pp. 105–118, Mar. 1989, <https://doi.org/10.3208/sandf1972.29.105>.

- [18] S. Iaf, K. Ichii, H. Liu, and T. Morita, "Effective Stress Analyses of Port Structures," *Soils and Foundations*, vol. 38, pp. 97–114, Sep. 1998, [https://doi.org/10.3208/sandf.38.Special\\_97](https://doi.org/10.3208/sandf.38.Special_97).
- [19] S. Iai, "Seismic Analysis and Performance of Retaining Structures," in *Geotechnical Earthquake Engineering and Soil Dynamics III*, Seattle, WA, USA, 1998, pp. 1020–1044.
- [20] I. Towhata and K. Ishihara, "Modelling soil behavior under principal stress axes rotation," in *International conference on numerical methods in geomechanics*, 1985, pp. 523–530.
- [21] B. O. Hardin and V. P. Drnevich, "Shear modulus and damping in soils: design equations and curves", Curves," *Journal of the Soil Mechanics and Foundations Division*, vol. 98, no. 7, pp. 667–692, Jul. 1972, <https://doi.org/10.1061/JSFEAQ.0001760>.
- [22] T. Morita, S. Iai, H. Liu, K. Ichi, and Y. Sato, "Simplified Method to Determine Parameter of FLIP," PARI Technical Note 0869, Jun. 1997.
- [23] I. Suetomi and N. Yoshida, "Nonlinear Behavior of Surface Deposit During the 1995 Hyogoken-Nambu Earthquake," *Soils and Foundations*, vol. 38, no. Special, pp. 11–22, 1998, [https://doi.org/10.3208/sandf.38.Special\\_11](https://doi.org/10.3208/sandf.38.Special_11).